





Communication

Synthesis of Pure Brookite Nanorods in a Nonaqueous Growth Environment

Mahmoud Hezam ^{1,*}, Saif M. H. Qaid ^{2,3}, Idriss M. Bedja ⁴, Fahhad Alharbi ^{5,6},
Mohammad Khaja Nazeeruddin ⁷ and Abdullah Aldwayyan ^{1,2}

¹ King Abdullah Institute for Nanotechnology, King Saud University, Riyadh 11451, Saudi Arabia; dwayyan@ksu.edu.sa

² Photonics Lab, Physics & Astronomy Department, King Saud University, Riyadh 11451, Saudi Arabia; sqaid@ksu.edu.sa

³ Department of Physics, Faculty of Science, Ibb University, P.O. Box 70270, Ibb, Yemen

⁴ Research Chair, Department of Optometry, College of Applied Medical Sciences, King Saud University, Riyadh 11433, Saudi Arabia; bedja@ksu.edu.sa

⁵ Electrical Engineering Department, King Fahd University of Petroleum and Minerals, Dhahran 31261, Saudi Arabia; fahhad.alharbi@kfupm.edu.sa

⁶ K.A. CARE Energy Research & Innovation Center, Dhahran 31261, Saudi Arabia

⁷ Group for Molecular Engineering of Functional Materials, Swiss Federal Institute of Technology Lausanne (EPFL), EPFL Valais Wallis, CH-1951 Sion, Switzerland; mdkhaja.nazeeruddin@epfl.ch

* Correspondence: mhezam@ksu.edu.sa

Received: 21 October 2019; Accepted: 24 October 2019; Published: 26 October 2019



Abstract: Brookite TiO₂ is the most difficult TiO₂ polymorph to synthesize. The available methods in the literature to produce brookite nanostructures mostly use water-based techniques for the preparation of water-soluble Ti complexes first, followed by a hydrothermal growth of the brookite nanostructures. Besides its multi-step nature, achieving a single brookite phase and optimizing the aqueous growth environment are all issues to be hardly controlled. In this work, pure brookite TiO₂ nanorods are synthesized using tetrabutyl titanate Ti(OBu)₄ and Sodium Fluoride (NaF) as precursor materials in a simple non-aqueous one-pot solvothermal process. Alcoholysis of only Ti(OBu)₄ in ethanol resulted in pure anatase nanoparticles, while the addition of NaF was essential to promote the growth of highly pure brookite nanorods. The phase purity is confirmed by X-Ray Diffraction, Raman Spectroscopy, and High-Resolution Transmission Electron Microscopy. The growth mechanism is explained according to the Ostwald's step rule, where Na⁺ ions are anticipated to have a potential role in driving the growth process towards the brookite phase.

Keywords: titanium dioxide; brookite; anatase; Raman

1. Introduction

Titanium dioxide (TiO₂) is a far-reaching multi-functional industrial material that has been in wide use for many significant applications such as photocatalysis, solar cells, cosmetics, pigments and protective coatings [1–8]. TiO₂ exists naturally in three crystalline phases: rutile, anatase and brookite. Rutile is the most stable bulk phase for TiO₂. At the nanoscale, the anatase phase is more stable, and abundant research outcomes have been reported on the growth of anatase TiO₂ nanostructures with various morphologies [8]. Stable rutile and brookite nanostructures, within a range of nanometer sizes, can also be realized under certain growth conditions [8–10]. Compared to rutile and anatase, the brookite phase is the least reported and is generally the most difficult to synthesize [11]. There have been many reported techniques for the synthesis of brookite nanostructures in an aqueous environment [12–23], most of which require very long growth times and several steps during the

growth process. Furthermore, some of the previously reported techniques result in multiphase nanostructures with mixed brookite/anatase or brookite/rutile TiO_2 phases, where a high control over the phase ratios and resulting morphologies is yet to be achieved [13,16–19]. Water-soluble complexes are usually used as titanium precursors, and the effect of growth parameters such as pH, temperature and complex ligands have been well addressed in the literature [12,18,20]. For example, it has been observed by many authors that the brookite phase is promoted under highly basic conditions [12,13]. Growth of brookite under acidic conditions has also been consistently reported when the water soluble Ti complexes are replaced by TiCl_4 [14,21–23]. The driving potential of the pH value and other parameters on the growth mechanism have thus been associated with different scenarios describing the possible mechanisms of brookite crystal growth [13,17,20–22]. Indeed, the use of a water-based growth environment has been a common denominator for most of the reported work on the growth of brookite nanostructures. Non-hydrolytic growth techniques, in which water is completely excluded from being both an oxygen donor and a reaction product, have proven to be very powerful for the synthesis of many oxide/mixed oxide nanostructures, providing simplified synthesis procedures and better control over the decomposition rates of reaction precursors [24,25]. However, reports on the growth of brookite TiO_2 in a non-hydrolytic environment are, up to the extent of our knowledge, very scarce. Buonsanti et al. reported a sophisticated surfactant-assisted nonaqueous method for the growth of pure brookite nanocrystals using high-temperature aminolysis of titanium carboxylate complexes [15]. Here, we report a greatly simplified one-pot synthesis of high-quality brookite nanorods in a purely nonaqueous environment. Our method is based on the direct alcoholysis of $\text{Ti}(\text{O}i\text{Bu})_4$ in ethanol in the presence of sodium fluoride (NaF) salt.

2. Materials and Methods

In a typical experiment, 12 g of $\text{Ti}(\text{O}i\text{Bu})_4$ (SigmaAldrich, 97%) and 1.48 g of NaF (SigmaAldrich, 99%) are mixed in 25 mL of anhydrous ethanol (SigmaAldrich, 99.8%) and vigorously stirred for 15 minutes at room temperature. The solution is then transferred to a 45 mL Teflon-lined stainless-steel autoclave and kept at 180 °C for 24 h. After the solvothermal reaction, the white precipitate is separated by high-speed centrifugation, washed with ethanol and distilled water several times and dried in an oven at 60 °C for ~6 h. No further calcination was performed on the samples. Another sample was also prepared without the addition of NaF to the growth solution. The grown samples were characterized using High Resolution Transmission Electron Microscopy (HRTEM) (JEOL JEM-2100F), Scanning Electron Microscopy (SEM) (JEOL-7600F), X-ray diffraction (XRD) (Xpert PAnalytical MPD), and Raman spectroscopy (B&W Tek i-Raman Plus, excitation wavelength: 532 nm).

3. Results and Discussion

Figure 1 shows the XRD patterns of the two samples: with and without the addition of NaF. Standard XRD reflection peaks of both brookite (JCPDS No. 29-1360) and anatase (JCPDS No. 21-1272) phases are also shown in the figure for comparison. The sample prepared with NaF could be fully indexed as pure brookite, while the non-NaF sample has a pure anatase phase. As can be observed in Figure 1, the anatase and brookite phases have many overlapping reflection positions. However, and as noted previously by Hu et al. [13], the anatase peak at a $2\theta = 62.7^\circ$ diffraction peak does not overlap with any of the brookite phase reflections, which confirms the pure brookite phase for the NaF-containing sample. As will be discussed below, both the HRTEM and Raman measurements additionally confirm the XRD conclusions.

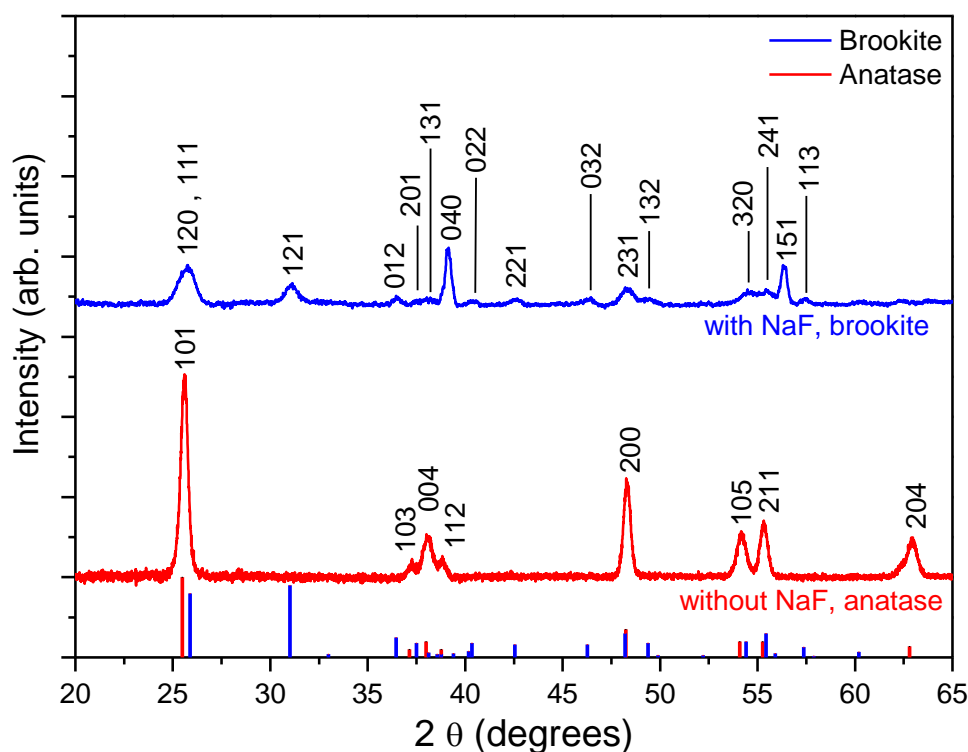


Figure 1. XRD patterns for the brookite (blue) and anatase (red) samples. The positions of the standard reflections for brookite (JCPDS No. 29-1360) and anatase (JCPDS No. 21-1272) are respectively shown as blue and red vertical bars at the bottom.

The TEM image for the grown brookite nanorods is shown in Figure 2a. Nanorods with diameters of ~10–20 nm and lengths of ~80–100 nm can be observed, along with smaller-size crystals. The small crystals have a brookite phase as well, as confirmed by the XRD and Raman results, and they possibly represent early nucleated crystals during the growth. Figure 2b shows a HRTEM image of single nanorods, and a portion of one nanorod (highlighted by a black rectangular frame) is further magnified in Figure 2c. The spacing between lattice fringes is measured to be 0.29 nm, corresponding to the (121) lattice spacing of the brookite structure. As both anatase and rutile (JCPDS No. 21-1276) structures do not have a similar lattice spacing, our data unambiguously confirms the brookite phase of the nanorod. The Fast Fourier Transform (FFT) pattern of the selected area is also plotted (in the inset of Figure 2c), confirming the single crystalline nature of the nanorod as well. Figure 2d shows an SEM micrograph of the grown nanorods. Growth without NaF resulted in pure anatase nanoparticles with no specific shape (Figure S1, ESI). It has to be pointed out that the two brookite XRD peaks at 38° (040) and 56° (151) closely coincide with the two highest NaF XRD peaks (JCPDS No. 36-1455) of (200) and (220) reflections respectively. Therefore, despite the careful washing of the growth product, the possibility of having NaF residuals cannot be excluded from the XRD results.

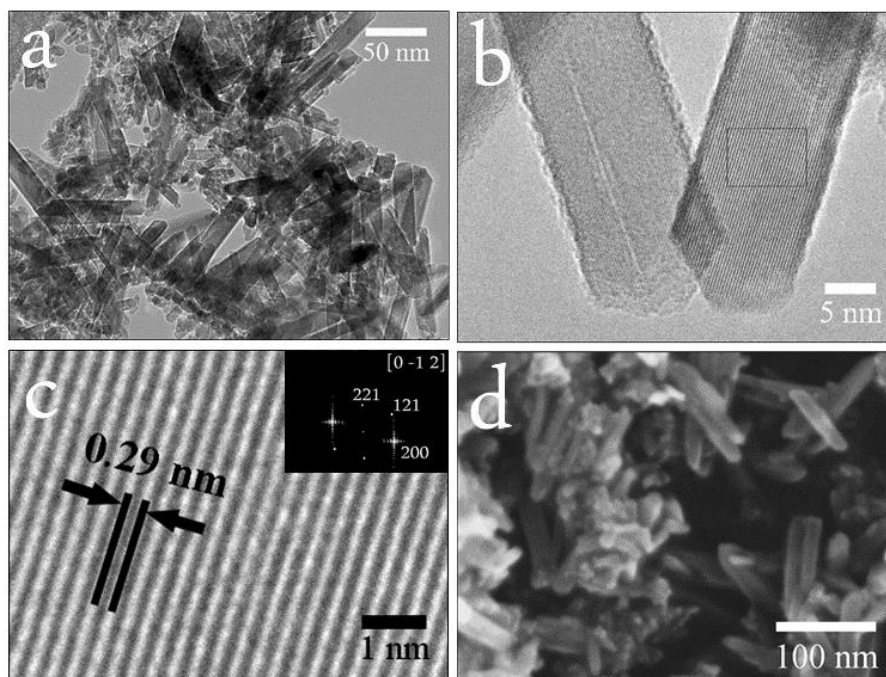
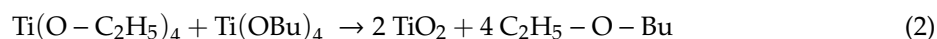
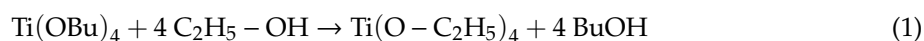


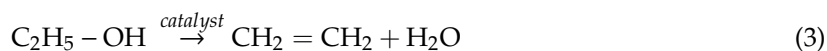
Figure 2. (a) TEM image of brookite nanorods; (b) HRTEM of brookite nanorods. The area inside the black frame is magnified in (c) and the FFT pattern is shown in the inset. The reflections in the FFT pattern could be indexed with a zone axis along the [0–12] direction. (d) SEM image of the grown brookite nanorods.

Figure 3 shows the Raman spectra for the grown nanostructures and confirms the assigned brookite and anatase phases to the NaF-containing and NaF-free samples respectively. For the NaF-containing sample, the brookite reflections at $\sim 149\text{ cm}^{-1}$, 196 cm^{-1} , 248 cm^{-1} , 326 cm^{-1} , 365 cm^{-1} , 406 cm^{-1} , 510 cm^{-1} , and 639 cm^{-1} can be identified [13]. On the other side, the NaF-free sample has the anatase reflections at 141 cm^{-1} , 194 cm^{-1} , 393 cm^{-1} , 515 cm^{-1} , and 636 cm^{-1} [26].

The solvothermal alcoholysis is proposed to follow the following reaction chain [24,27]:



In this scenario, the reaction will result in butanol (BuOH) and butyl ethyl ether ($\text{C}_2\text{H}_5 - \text{O} - \text{Bu}$) as byproducts, implying a completely water-free growth environment. Among all possible unary and binary reactions of the chemical ingredients in use, the only reaction that can possibly result in water as a by-product is the direct dehydration of ethanol under high temperature, which results in ethylene and water as follows:



This reaction is also not likely to take place, as it requires either a powder catalyst, e.g., Al_2O_3 , or a concentrated acid catalyst, e.g., H_2SO_4 , to be stimulated [28,29]. Therefore, the reaction environment can be confirmed to be purely non-hydrolytic.

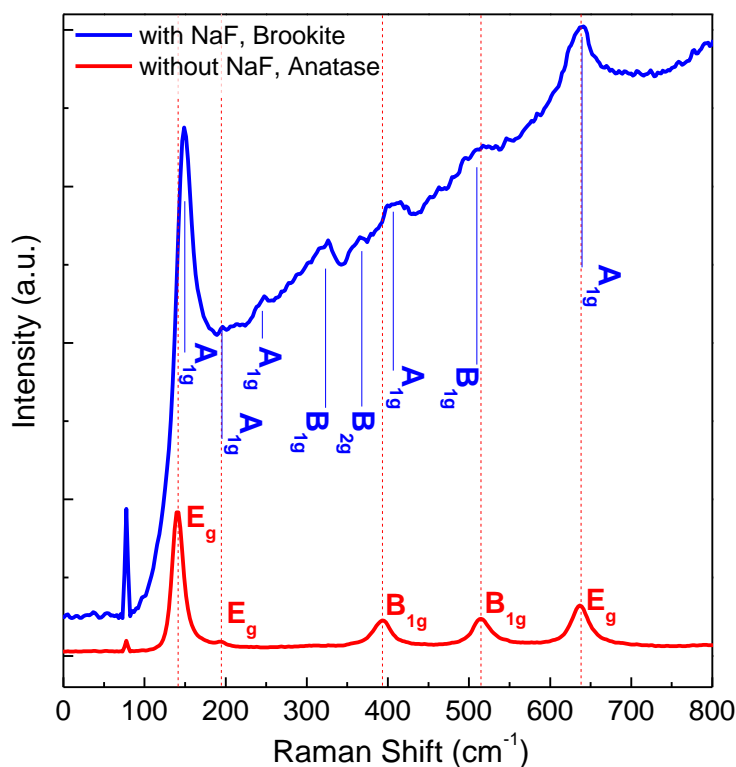


Figure 3. Raman spectra for the grown brookite (blue) and anatase (red) samples. The anatase Raman reflections are further clarified by vertical dashed red lines.

The available literature is dominated by brookite grown in water-based environments, and it is already very divergent when it comes to explaining the growth mechanism [13,17,20–22,30]. Indeed, a growth mechanism is even more difficult to establish in our case, especially with the possible presence of different organic compounds during the growth. However, some insights can be concluded, especially regarding the importance of sodium ions in the brookite phase formation. First, $\text{Ti}(\text{OBU})_4$ is a well-known commercial organic Ti precursor that has been widely used for the growth of the anatase phase using both water and alcohol solvents or a mixture of both [31–33]. On another side, hydrogen fluoride acid (HF) has been reported to play a vital role to promote the growth of anatase nanosheets with exposed {001} facets using $\text{Ti}(\text{OBU})_4$ as a precursor, and using other Ti precursors as well, in purely non-hydrolytic growth environments [34]. Both theoretical and experimental evidence confirmed the strong role of F^- ions to lower the high surface energy of {001} facets and thus promoted such nanosheet morphology [34–36]. Here, with the use of NaF, the role of Na^+ ions is clearly dominated that of F^- ions for two reasons. First, despite the strong role reported for F^- ions to promote the anatase phase with exposed {001} facets, no anatase phase was formed. Second, Na^+ ions have been found by many authors, using water-based environments, to have a crucial role in promoting the growth of the brookite phase. Among all other growth parameters, the presence of Na^+ ions was reported to be the primary parameter for realizing the brookite phase [13,17]. For example, despite the fact that the formation of the brookite phase takes place only at pH values of 12 or higher, the brookite phase does not form at all when NaOH is replaced by other bases such as LiOH and KOH [13]. The existence of Na^+ ions is thus, as shown by our results and the above-mentioned reports, a fundamental factor to promote the brookite phase. The subsequent processes can then be explained as follows. Upon the solvothermal alcoholysis process (Equations (1) and (2)), TiO_6^- octahedra will form, which have a condensation process that can go through intermediate metastable steps following the Ostwald's step rule [37,38]. As widely adopted by many authors [13,17,30], TiO_6^- octahedra will condensate first into 2D anionic sheets of layered titanate before a structural transformation takes place. Positive ions in the

solution can intercalate between the negatively charged titanate layers, and the electrostatic interaction will cause the metastable layered structure to temporarily stabilize. The main challenge after that is to drive the subsequent crystallization process into the required stable crystalline form (rutile, anatase or brookite). Of course, different ions will stabilize the layered titanate structure differently and can therefore result in different structural transformations. In this regard, Na⁺ ions are obviously unique in driving the crystallization process into the brookite phase pathway rather than anatase or rutile, a fact that is shown by our results and that has been found to hold, as mentioned above, in water-based environments as well.

4. Conclusions

In summary, pure brookite nanorods were successfully grown in a water-free growth environment. The brookite phase of the nanorods was confirmed by XRD, Raman and HRTEM measurements. The growth mechanism is explained according to the Ostwald's step rule, where Na⁺ ions stabilizes the initially formed 2D titanate sheets in a way that prefers subsequent crystallization into the brookite phase.

Supplementary Materials: The following are available online at <http://www.mdpi.com/2073-4352/9/11/562/s1>, Figure S1: TEM and HRTEM images of the NaF-free anatase sample

Author Contributions: M.H. and S.M.H.Q performed the experiments. S.M.H.Q. provided original draft preparation. M.H. wrote the manuscript. I.M.B., F.A., M.K.N. and A.A. assisted in the experimental design and manuscript editing. A.A. provided overall project administration.

Funding: This Project was funded by the National Plan for Science, Technology and Innovation (MAARIFAH), King Abdulaziz City for Science and Technology, Kingdom of Saudi Arabia, Award Number (11-ENE1474-02).

Conflicts of Interest: The authors declare no conflict of interest.

References

1. Fujishima, A.; Rao, T.N.; Tryk, D.A. Titanium dioxide photocatalysis. *J. Photochem. Photobiol. C Photochem. Rev.* **2000**, *1*, 1–21. [[CrossRef](#)]
2. Daghri, R.; Drogui, P.; Robert, D. Modified TiO₂ For Environmental Photocatalytic Applications: A Review. *Ind. Eng. Chem. Res.* **2013**, *52*, 3581–3599. [[CrossRef](#)]
3. Ghathan, H.M.; Qaid, S.M.H.; Hezam, M.; Labis, J.P.; Alduraibi, M.; Bedja, I.M.; Aldwayyan, A.S. Laser induced photocurrent and photovoltage transient measurements of dye-sensitized solar cells based on TiO₂ nanosheets and TiO₂ nanoparticles. *Electrochim. Acta.* **2016**, *212*, 992–997. [[CrossRef](#)]
4. Nazeeruddin, M.K.; Péchy, P.; Renouard, T.; Zakeeruddin, S.M.; Humphry-Baker, R.; Cointe, P.; Liska, P.; Cevey, L.; Costa, E.; Shklover, V.; et al. Engineering of efficient panchromatic sensitizers for nanocrystalline TiO₂-based solar cells. *J. Am. Chem. Soc.* **2001**, *123*, 1613–1624. [[CrossRef](#)]
5. Giordano, F.; Abate, A.; Correa Baena, J.P.; Saliba, M.; Matsui, T.; Im, S.H.; Zakeeruddin, S.M.; Nazeeruddin, M.K.; Hagfeldt, A.; Graetzel, M. Enhanced electronic properties in mesoporous TiO₂ via lithium doping for high-efficiency perovskite solar cells. *Nat. Commun.* **2016**, *7*, 10379. [[CrossRef](#)]
6. Popov, A.P.; Priezzhev, A.V.; Lademann, J.; Myllylä, R. TiO₂ nanoparticles as an effective UV-B radiation skin-protective compound in sunscreens. *J. Phys. D. Appl. Phys.* **2005**, *38*, 2564–2570. [[CrossRef](#)]
7. Braun, J.H.; Baidins, A.; Marganski, R.E. TiO₂ pigment technology: a review. *Prog. Org. Coatings* **1992**, *20*, 105–138. [[CrossRef](#)]
8. Chen, X.; Mao, S.S. Titanium dioxide nanomaterials: Synthesis, properties, modifications and applications. *Chem. Rev.* **2007**, *107*, 2891–2959. [[CrossRef](#)]
9. Zhang, H.; Banfield, J.F. Thermodynamic analysis of phase stability of nanocrystalline titania. *J. Mater. Chem.* **1998**, *8*, 2073–2076. [[CrossRef](#)]
10. Zhang, H.; Banfield, J.F. Understanding Polymorphic Phase Transformation Behavior during Growth of Nanocrystalline Aggregates: Insights from TiO₂. *J. Phys. Chem. B* **2000**, *104*, 3481–3487. [[CrossRef](#)]
11. Paola, A. Di; Bellardita, M.; Palmisano, L. *Brookite, the Least Known TiO₂ Photocatalyst*, 2013; Volume 3, ISBN 3909170250.

12. Kobayashi, M.; Petrykin, V.; Tomita, K.; Kakihana, M. Hydrothermal synthesis of brookite-type titanium dioxide with snowflake-like nanostructures using a water-soluble citratoperoxotitanate complex. *J. Cryst. Growth* **2011**, *337*, 30–37. [[CrossRef](#)]
13. Hu, W.; Li, L.; Li, G.; Tang, C.; Sun, L. High-quality brookite TiO₂ flowers: Synthesis, characterization, and dielectric performance. *Cryst. Growth Des.* **2009**, *9*, 3676–3682. [[CrossRef](#)]
14. Kuznetsova, I.N.; Blaskov, V.; Stambolova, I.; Znaidi, L.; Kanaev, A. TiO₂ pure phase brookite with preferred orientation, synthesized as a spin-coated film. *Mater. Lett.* **2005**, *59*, 3820–3823. [[CrossRef](#)]
15. Buonsanti, R.; Grillo, V.; Carlino, E.; Giannini, C.; Kipp, T.; Cingolani, R.; Cozzoli, P.D. Nonhydrolytic synthesis of high-quality anisotropically shaped brookite TiO₂ nanocrystals. *J. Am. Chem. Soc.* **2008**, *130*, 11223–11233. [[CrossRef](#)]
16. Kandiel, T.A.; Feldhoff, A.; Robben, L.; Dillert, R.; Bahnemann, D.W. Tailored titanium dioxide nanomaterials: anatase nanoparticles and brookite nanorods as highly active photocatalysts. *Chem. Mater.* **2010**, *22*, 2050–2060. [[CrossRef](#)]
17. Yang, M.-H.; Chen, P.-C.; Tsai, M.-C.; Chen, T.-T.; Chang, I.-C.; Chiu, H.-T.; Lee, C.-Y. Anatase and brookite TiO₂ with various morphologies and their proposed building block. *Cryst. Eng. Comm.* **2014**, *16*, 441–447. [[CrossRef](#)]
18. Yoshizawa, M.; Kobayashi, M.; Petrykin, V.; Kato, H.; Kakihana, M. Insights into a selective synthesis of anatase, rutile, and brookite-type titanium dioxides by a hydrothermal treatment of titanium complexes. *J. Mater. Res.* **2014**, *29*, 90–97. [[CrossRef](#)]
19. Xu, H.; Zhang, L. Controllable one-pot synthesis and enhanced photocatalytic activity of mixed-phase TiO₂ nanocrystals with tunable brookite/rutile ratios. *J. Phys. Chem. C* **2009**, *113*, 1785–1790. [[CrossRef](#)]
20. Kobayashi, M.; Tomita, K.; Petrykin, V.; Yoshimura, M.; Kakihana, M. Direct synthesis of brookite-type titanium oxide by hydrothermal method using water-soluble titanium complexes. *J. Mater. Sci.* **2008**, *43*, 2158–2162. [[CrossRef](#)]
21. Pottier, A.; Chanéac, C.; Tronc, E.; Mazerolles, L.; Jolivet, J.-P. Synthesis of brookite TiO₂ nanoparticles by thermolysis of TiCl₄ in strongly acidic aqueous media. *J. Mater. Chem.* **2001**, *11*, 1116–1121. [[CrossRef](#)]
22. Lin, H.; Li, L.; Zhao, M.; Huang, X.; Chen, X.; Li, G.; Yu, R. Synthesis of high-quality brookite TiO₂ single-crystalline nanosheets with specific facets exposed: Tuning catalysts from inert to highly reactive. *J. Am. Chem. Soc.* **2012**, *134*, 8328–8331. [[CrossRef](#)] [[PubMed](#)]
23. Lee, B.I.; Wang, X.; Bhave, R.; Hu, M. Synthesis of brookite TiO₂ nanoparticles by ambient condition sol process. *Mater. Lett.* **2006**, *60*, 1179–1183. [[CrossRef](#)]
24. Vioux, A. Nonhydrolytic Sol-Gel Routes to Oxides. *Chem. Mater.* **1997**, *9*, 2292–2299. [[CrossRef](#)]
25. Debecker, D.P.; Mutin, P.H. Non-hydrolytic sol-gel routes to heterogeneous catalysts. *Chem. Soc. Rev.* **2012**, *41*, 3624. [[CrossRef](#)] [[PubMed](#)]
26. Zhang, W.F.; He, Y.L.; Zhang, M.S.; Yin, Z.; Chen, Q. Raman scattering study on anatase TiO₂ nanocrystals. *J. Phys. D. Appl. Phys.* **2000**, *33*, 912–916. [[CrossRef](#)]
27. Bian, Z.; Zhu, J.; Li, H. Solvothermal alcoholysis synthesis of hierarchical TiO₂ with enhanced activity in environmental and energy photocatalysis. *J. Photochem. Photobiol. C Photochem. Rev.* **2016**, *28*, 72–86. [[CrossRef](#)]
28. Takahara, I.; Saito, M.; Inaba, M.; Murata, K. Dehydration of ethanol into ethylene over solid acid catalysts. *Catal. Letters* **2005**, *105*, 249–252. [[CrossRef](#)]
29. Xu, X.; Almeida, C. De; Antal, M.J. Mechanism and kinetics of the acid-catalyzed dehydration of ethanol in supercritical water. *J. Supercrit. Fluids* **1990**, *3*, 228–232. [[CrossRef](#)]
30. Nagase, T.; Ebina, T.; Iwasaki, T.; Hayashi, K.; Onodera, Y.; Chatterjee, M. Hydrothermal synthesis of brookite. *Chem. Lett.* **1999**, 911–912. [[CrossRef](#)]
31. Zhou, W.; Liu, X.; Cui, J.; Liu, D.; Li, J.; Jiang, H.; Wang, J.; Liu, H. Control synthesis of rutile TiO₂ microspheres, nanoflowers, nanotrees and nanobelts via acid-hydrothermal method and their optical properties. *Cryst. Eng. Comm.* **2011**, *13*, 4557. [[CrossRef](#)]
32. Sifang, L.; Guoliang, Y.; Guoqin, C. Low-temperature preparation and characterization of nanocrystalline anatase TiO₂. *J. Phys. Chem. C* **2009**, *113*, 4031–4037.
33. Kominami, H.; Kato, J.I.; Murakami, S.Y.; Kera, Y.; Inoue, M.; Inui, T.; Ohtani, B. Synthesis of titanium(IV) oxide of ultra-high photocatalytic activity: High-temperature hydrolysis of titanium alkoxides with water liberated homogeneously from solvent alcohols. *J. Mol. Catal. A Chem.* **1999**, *144*, 165–171. [[CrossRef](#)]

34. Han, X.; Kuang, Q.; Jin, M.; Xie, Z.; Zheng, L. Synthesis of titania nanosheets with a high percentage of exposed (001) facets and related photocatalytic properties. *J. Am. Chem. Soc.* **2009**, *131*, 3152–3153. [[CrossRef](#)] [[PubMed](#)]
35. Yu, J.C.; Yu, J.; Ho, W.; Jiang, Z.; Zhang, L. Effects of F- doping on the photocatalytic activity and microstructures of nanocrystalline TiO₂ powders. *Chem. Mater.* **2002**. [[CrossRef](#)]
36. Yang, H.G.; Sun, C.H.; Qiao, S.Z.; Zou, J.; Liu, G.; Smith, S.C.; Cheng, H.M.; Lu, G.Q. Anatase TiO₂ single crystals with a large percentage of reactive facets. *Nature* **2008**, *453*, 638–641. [[CrossRef](#)] [[PubMed](#)]
37. Ostwald, W. Studien über die Bildung und Umwandlung fester Körper. *Zeitschrift für Phys. Chemie.* **1897**, *22*, 289–330. [[CrossRef](#)]
38. Van Santen, R.A. The Ostwald step rule. *J. Phys. Chem.* **1984**, *88*, 5768–5769. [[CrossRef](#)]



© 2019 by the authors. Licensee MDPI, Basel, Switzerland. This article is an open access article distributed under the terms and conditions of the Creative Commons Attribution (CC BY) license (<http://creativecommons.org/licenses/by/4.0/>).